Biosensors and Bioelectronics 141 (2019) 111414

Contents lists available at ScienceDirect

Biosensors and Bioelectronics

journal homepage: www.elsevier.com/locate/bios

Coaxial sensing bio-amplifier for ultrasensitive detections of circulating tumor DNAs

Zhen Zhang[b,1,2], Mengting Zhu[a,b,1,2], Zichao Chen[b,2], Xiaomeng Wang[b,2], Guang Chen[a,**,2], Shusheng Zhang[b,*,2]

[a] Shandong Province Key Laboratory of Life Organic Analysis, College of Chemistry and Chemical Engineering, Qufu Normal University, Qufu, 273165, PR China
[b] Shandong Province Key Laboratory of Detection Technology for Tumor Markers, College of Chemistry and Chemical Engineering, Linyi University, Linyi, 276000, PR China

ARTICLE INFO

Keywords:
Coaxial sensing
Circulating tumor DNA
3D amplifier
Catalytic bio-nanofiber
DNA replication programming

ABSTRACT

We herein report the first attempt to engineer a coaxial-sensing 3D amplifier able to achieve dynamic self-assembly in response to a mutated-ctDNA target. A bio-nanofiber is firstly manufactured via an ingenious double-channel electrostatic spinning and DNA rolling circle replication (RCR) technology, which offered an ideal scaffold for assembly of 3D amplifier activated by target recognition. The coaxial-controllable signal amplifier presented several advantages. (1) Given its "coaxial sensing effect", the proposed bio-amplifier played the coaxial transduction for signal enrichment to vastly increase sensitivity, capable of discriminating a single-base mismatched sequence from the perfectly complementary one, using ctDNA-134A as a model analyte. (2) Due to "covalent bridges lock effect" in an identifying chip with locked nucleic acid beacons, this 3D amplifier expressed high specificity and biostability toward seven different mutated-ctDNAs. (3) Profiting from special configuration of bioactive nanofibers and DNA replication programming, this catalytic bio-amplifier possessed "signal enrichment effect", which enhanced dynamic range toward ctDNA-134A detection and hybridized without any external indicators. This innovative bio-amplifier has a detection limit of 5.1 aM for ctDNA-134A with superior specificity, excellent sensitivity, and good performance. This pioneered method was further applied for broadly differentiate cells and evaluate changes in the expression levels of intracellular mutated-ctDNAs.

1. Introduction

Tumor is in essence a typical genetic disease induced by gene mutation (Hanahan and Weinberg. 2011; Angulo et al., 2013; Catherine et al., 2013). Although tumor biopsies are currently the most dependable ways for clinical application of cancer diagnose, they are sadly invasive and frequently difficult to achieve. Even if biopsies can be gained, missed diagnoses are still possible due to the heterogeneity and continuous evolution of tumor (Harley, 2008; Murtaza et al., 2013). Circulating tumor DNA (ctDNA), as an effective tumor-related biomarker, the levels of ctDNA in blood of neoplasm patients have been closely connected with cancer burden and malignant progression, potentially replacing tissue biopsies in certain diagnostic applications, has attracted increasing attentions for developing a noninvasive cancer assessment of clinical significance (Newman et al., 2014; Abbosh et al., 2017; Kaiser, 2010; Xu et al., 2017).

The conventional approaches of ctDNA assay primarily involve DNA sequencing and polymerase chain reaction (PCR) (Kaiser, 2010; Garcia-Olmo et al., 2010; Cutsem et al., 2011). Despite these PCR technologies resulting in meaningful contributions to ctDNA determination, there remain sufficiently challenging in clinical practice: highly skilled droplets are inconvenient, volume samples are large (> 3 mL), and trace analysis is vulnerable to interference from the constituents of the complex biological environment (Quick et al., 2017; Siravegna et al., 2017; Garcia-Olmo et al., 2010). Microfluidic technology is also an effective method for the detection of tumor markers. It can use microfluidic chip design to specifically identify and capture circulating tumor cells for detection. When analyzing cell aggregates, it can

* Corresponding author.
** Corresponding author.
E-mail addresses: chenandguang@163.com (G. Chen), shushzhang@126.com (S. Zhang).
[1] Zhen Zhang (Z. Zhang) and Mengting Zhu (M. T. Zhu) contributed equally to this work.
[2] All authors contribute equally.

https://doi.org/10.1016/j.bios.2019.111414
Received 19 April 2019; Received in revised form 2 June 2019; Accepted 4 June 2019
Available online 05 June 2019
0956-5663/

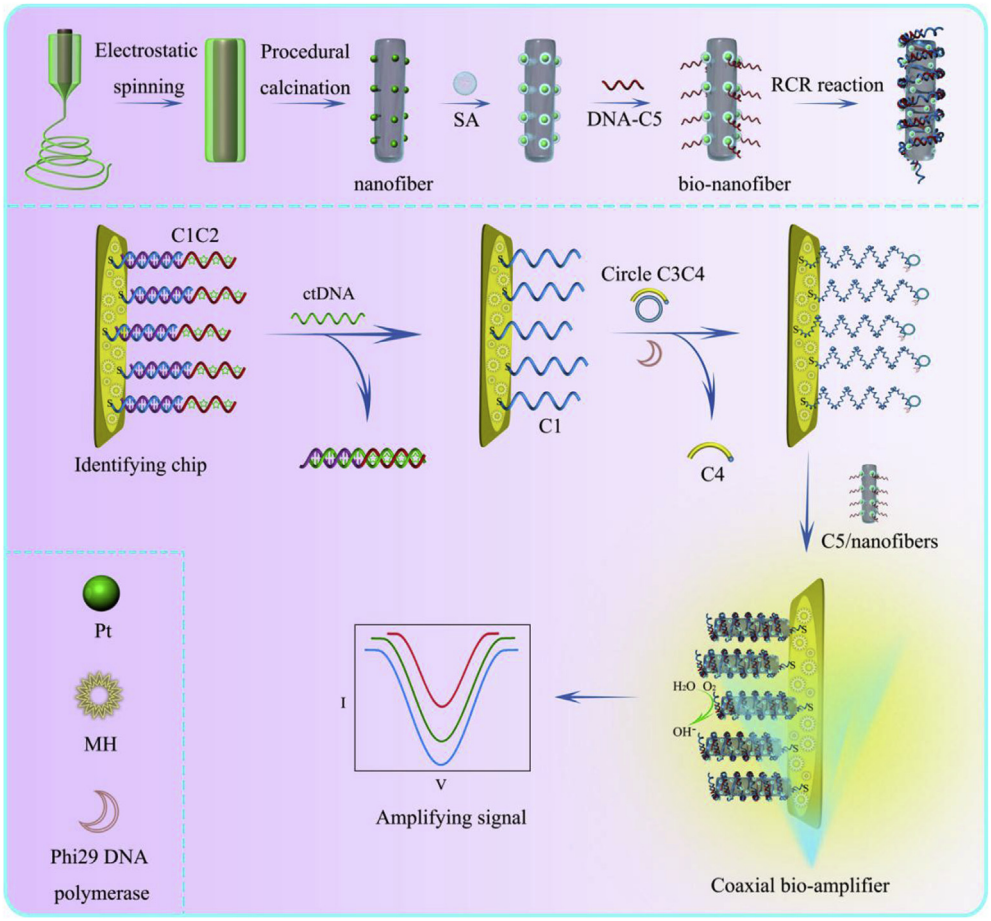

Fig. 1. Illustration of coaxial sensing bio-amplifier for monitoring the mutated ctDNAs based on a novel 3D bio-nanofiber.

accurately represent the variation between cells (Guan et al., 2014; Song et al., 2017). But the chip design is commonly complicated and the accuracy requirement is high. DNA sequencing, containing next-generation sequencing offer a highly sensitive and selective technique, nevertheless, there is no possibility to meet the demand of rapid diagnosis and first-line therapy of metastatic diseases, due to the very long-time process in acquiring sequence information (normally 10–20 days) (Garcia-Olmo et al., 2010; Cutsem et al., 2011). Especially, ctDNA has a short half-life which is less than 2 h in blood, so it may provide a much clearer survey of the tumor's present rather than its past. The timely monitoring mutated ctDNAs in blood of tumor patient is enormously challenging, since infinitesimal ctDNAs are often accompanied with abundant wide-type DNAs of high abundance ratios (Abbosh et al., 2017; Xu et al., 2017; Diehl et al., 2008). Hence, for successfully monitoring the mutated ctDNAs, it is of great significance to detect mutated ctDNAs at the extremely low-levels in patient samples, with rapid response, simple operation process, high sensitivity and accuracy, in the company of high-level interferences of unmutated sequences (Xu et al., 2017; Gorgannezhad et al., 2018; Hu et al., 2018).

Nucleic acids have been regarded as promising design modules to construct various kinds of highly ordered structures and devices due to sequence programmability and specific identifiability (Li et al., 2017; Liu et al., 2018b; Stulz et al., 2011), with multifarious sizes and spatial structures such as silicified DNA origami (Liu et al., 2018b), valency-controlled framework nucleic acids (Liu et al., 2018a), DNA lattices (Manuguerra et al., 2017), DNA origami (Jabbari et al., 2015), DNA tetrahedron structures (Lin et al., 2015), DNA nanotubes (Mohammed et al., 2017), etc. Meanwhile, these innovative nucleic-acid technologies have stimulated substantial research efforts in the fields for detecting various miRNA, DNA or proteins targets (Mohammed et al., 2017; Zhang et al. 2016, 2017; Wang et al., 2015). Whereas challenges generally persist. Traditional nucleic-acid structures were usually based on a unidirectional sensing mode, which typically reveals the limited specificity and sensitivity for intracellular monitoring low-abundance biomolecules. Currently, locked nucleic acids (LNAs) as a nucleotide derivative, have been considered as an ideal tool for single nucleotide polymorphism analysis owing to their unique property. They have covalent bridges to “lock” the ribose in the N-type (3-endo) conformation, to have prominent superiorities such as outstanding mismatch recognition capacity, high base-pairing ability and binding strength for complementary DNA or RNA sequences (Obernosterer et al., 2007; Straarup et al., 2010). Thus, the development of LNA/DNA molecules targeting-technology with multipath effects is urgently expected to overcome these restrictions.

Inspired by the nature of coaxial inorganic-materials (Loscertales et al., 2002; Zhao et al., 2007; Ji et al., 2015), a novel coaxial sensing biomaterial with multipath effects was prepared by dynamic self-assembly of nucleic acids on the ordered scaffolds. This unique 3D bio-nanofiber (3BF) was *in situ* generated on an identifying chip, as a 3D sensing bio-amplifier, which possesses of superior biocompatibility, space effect and bio-stability, particularly inherent coaxial biosensing performance. Simultaneously, this identifying chip with locked nucleic acid beacons (LNB) of tumor-specific mutation, with remarkable recognition ability of single-base, was manufactured for monitoring the mutated-ctDNAs in peripheral blood. A coaxial sensing amplifier was successfully constructed to detect the mutated ctDNAs in cancer cells for the first time, by the significant synergies of LNB and *in situ* 3BF on the chip. This innovative bio-amplifier displayed excellent specificity, high sensitivity with the detection limit of 5.1 aM for ctDNA-134A, and worthy performance in human serum assay.

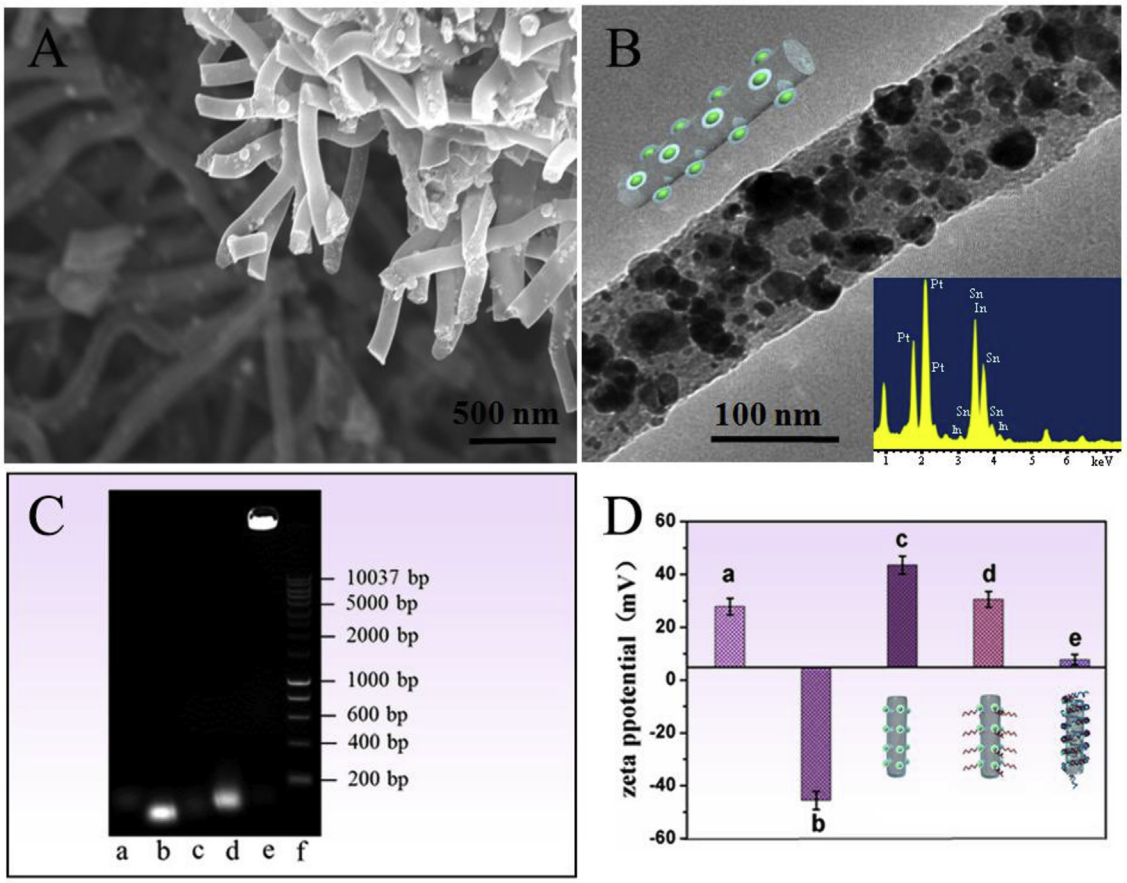

Fig. 2. (A) SEM image of Pt/ITO nanofibers. (B) TEM image of Pt/ITO nanofibers, Inset: EDS spectrum of Pt/ITO nanofibers. (C) The RCR reaction was analyzed by 1.0% agarose gel electrophoresis: C1 (b), C2 (c), C3 (a), circle C3C4 (d), the RCR products (e), and the marker (f). (D) ZP analysis of Pt/ITO nanofibers (a), TA-Pt/ITO (b), SA-Pt/ITO (c), C5-nanofibers (d), 3D bio-nanofibers (e).

2. Experimental section

2.1. Reagents and apparatus

Indium (III) nitrate hydrate,6-Mercapto-1-hexanol (MH), Polyvinyl pyrrolidone (PVP), streptavidin (SA), Stannic chloride hydrated, K_2PtCl_6, Indium(III) acetate, thioglycolic acid (TA), and Tris(2-carboxyethyl) phosphine (TCEP) were obtained from Aladdin and used directly. QIAmp®DNA Mini Kit was gained from Qiagen. PBS was purchased from Aladdin. The ultrapure water (≥18.25 MΩ) acquired by the Millipore water purification system was used throughout the experiment. The whole experiment was carried out on a laminar flow stage to ensure a clean environment to control the effect of RNase. Phi29 DNA polymerase, T4 DNA ligase and deoxynucleotide solution mixture (dNTPs) were ordered from TaKaRa Biotechnology (Dalian) Co.,Ltd. All of the nuclear acids including target Kirsten sarcoma-2 virus (KSV) mutations, wide type KS2V allele, complementary strands of wild type KSV allele, capture DNAs were purified by high-performance liquid chromatography from Sangon Biotech Co., Ltd. (Shanghai, China), and their detailed sequences are listed in Tables S1 and S2.

Transmission electron microscopy (TEM) images and energy dispersions X-ray spectroscopy (EDX) spectral data were provided by a JEM-2100 machine (JEM-2100, Hitachi, Japan). Zeta potentials were procured from Nano ZS90 (Malvern, UK). Fluorescence images were gained by fluorescent inverted microscope (NiKON 660E). All of the measurements of cyclic voltammetry (CV) and differential pulse voltammetry (DPV) and the electrochemical impedance spectroscopy (EIS) based on nanofibers were implemented on a CHI 660E electrochemical analyzer (CH Instruments, Shanghai) at room temperature, a modified Au-chip of coaxial bio-nanofibers as the working chip.

2.2. Preparation of nano-composite fibers

First, 0.5 g $In(NO_3)_3{\cdot}4.5H_2O$, 0.1 g $SnCl_4{\cdot}5H_2O$, and 1.903 g PVP were dissolved in 9.50 g DMF, and magnetically stirred at room temperature for 6 h to acquire a uniform, clear, stable mucus. Second, two types of sols were respectively taken into two syringe-channels with an in-line needle of stainless steel in the electrospinning equipment. A grounding plate with tin foil as a receiver, there adjusted the distance between this plate and the needle to 17 cm, and the spinning voltage was 18 kV. Third, composite fiber-membranes were got and placed in an oven at 70 °C for 12 h, the black fiber-membranes were moved into a tube furnace, the temperature was raised to 800 °C at 2 °C/min. Finally, there was calcined for 2 h and then naturally cooled to room temperature, and then Pt/ITO nanofibers were successfully achieved.

2.3. Preparation of LNB-chip and DNA-chip

A neat Au-chip was soaked in DNA-C1 liquor involving TCEP for 10 h. DNA-C1 with thiol-groups was activated to conjugate with the Au-chips, in the shape of S–Au bonds by TCEP catalysis. After the surface of the C1-chips blocked by MH, there entirely swashed with PBS to dispose of needless C1. The C1-chip was rinsed with buffer solution, and then C2 modified with locked nucleic acids were cross-fertilized with C1-chip at 37 °C for 3 h. The LNB-chip was generated after washed with buffer solution. For subsequent contrast tests, C6 (DNA sequences) was cross-fertilized with C1-chip to get a DNA-chip.

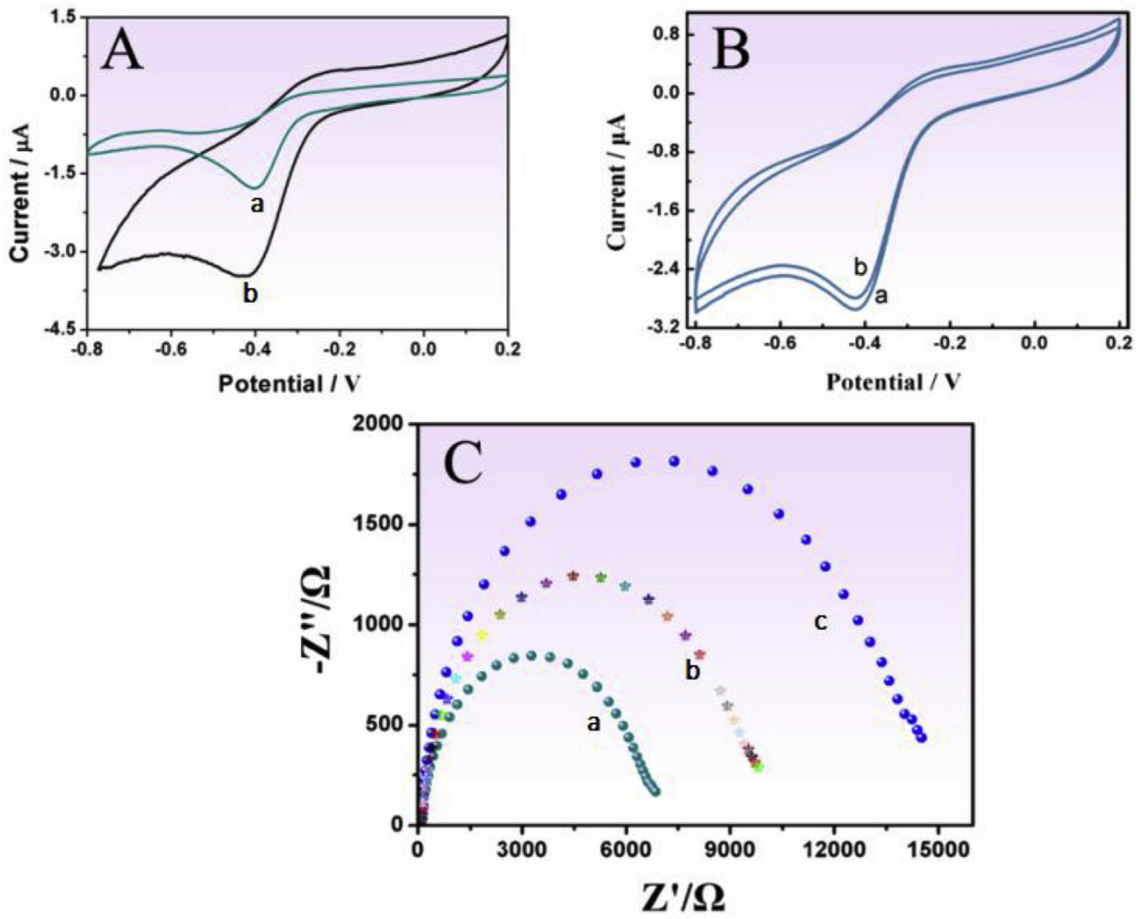

Fig. 3. (A) CVs of Pt nanoparticles (a), Pt/ITO nanofibers (b) in 0.1 M KOH of oxygen saturation. (B) CVs contrast of Pt/ITO nanofibers between −0.8 and 0.2 V of before and after 200 cycles in 0.1 M KOH of oxygen saturation. (C) Nyquist plots recorded at Pt/ITO nanofibers (a), C5-nanofibers (b), 3D bio-nanofibers (c) in oxygen-saturated PBS (0.1 M, pH 7.6).

2.4. Assembly of 3D bio-nanofiber

The LNB-chip was dipped in a solution involving the specific target-ctDNA. After washed with buffer solution, phi29 DNA polymerase and circle-DNA (C3C4) were injected to stimulate the rolling circle amplification reaction at 37 °C for 240 min, to get the R-chip. Secondly, R-chip was incubated in the solution of C5/nanofibers in constant temperature shaker for 180 min. After cleanout with buffer solution, 3D bio-nanofibers were successfully assembled on the chip.

2.5. Cell culture and DNA extraction

A549, LOVO, MCF-7, HepG2 cells and LO2 cells were cultured in DMEM medium with 10% fetal bovine serum and 1% penicillin-streptomycin, and allowed to humidify cells at 37 °C in a humidified atmosphere with 5% CO_2, in accordance with the protocol of American type culture collection. These cells were harvested after 48 h of incubation and washed three times with PBS (10 mM, pH 7.4) and counted with a cell counter. Nucleic acids in cells were extracted by QIAmp®DNA Mini Kit on the basis of operation instructions. After adding R Nase A, RNAs in nucleic acids were digested at 37 °C for 15 min. The obtained products were prepared for the subsequent experiments.

3. Results and discussion

3.1. Design for coaxial sensing bio-amplifier to monitor the mutated ctDNAs

In this study, a coaxial sensing bio-amplifier *via* the proper synergy between an identifying chip and 3D bio-nanofiber was proposed with the remarkable specificity and sensitivity (Fig. 1). This catalyzed DNA-amplifier was applied as a versatile amplification platform to analyze nucleic acids applying ctDNA as a model analyte. By evolving recognition response into electrochemical coaxial transduction, we introduced a signal-on strategy to successfully achieve the detection of low amount of ctDNA. The mechanism pathways were described as follows. First, LNB of tumor-specific mutation were ingeniously prepared on the chip, and then MH was used to block the surface of chip for removing unspecific adsorption. It could serve not only as a probe to accurately discriminate the mutated ctDNAs with similar sequences but also as a primer for DNA rolling circle replication (RCR) reaction. Second, C1-ssDNA (Table S2) as a primer were uncovered by adding target ctDNA and got free in the identifying chip. And then C1-ssDNA hybridized with circle C3C4, C4 with 3′-NH_2 blocked group broke away from this circle, which would activate the RCR reaction in the presence of dNTPs and Phi29 DNA polymerase (Fig. S1). Nanofibers and C5 assembled via the strong biotin-streptavidin (SA) interaction. Third, it would stimulate a large number of C5/nanofibers to hybridize with the RCR product (end product of RCR amplification). 3D bio-nanofibers employed a unique structure by the significant synergies of RCR product and C5/nanofibers (Fig. 2) with electrochemical coaxial transduction. As a result, abundant signal probes could be fastened on the specific chip. After self-assembly of the catalyzed coaxial bio-amplifier, the mutated ctDNAs as the target analyte could be recognized by measuring the signal from coaxial DNA-amplifier fastened on the chip. Aiming at seven KSV point mutations, it could be avoided by employing the functional chip as supporter that the excess signal-barcodes caused

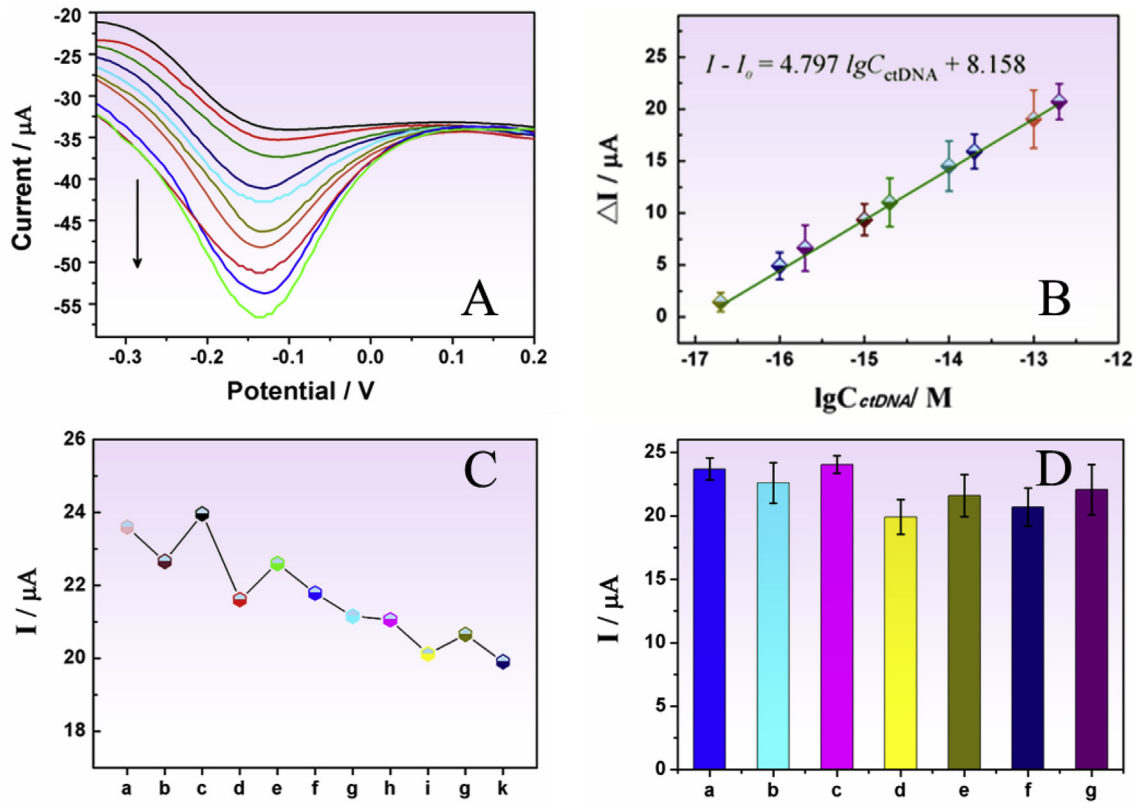

Fig. 4. (A) DPV response changes in response to different concentrations of target ctDNA-134A: 0 M, 2.0×10^{-17} M, 1.0×10^{-16} M, 2.0×10^{-16} M, 1.0×10^{-15} M, 2×10^{-15} M, 10^{-14} M, 2×10^{-14} M and 10^{-13} M, 2×10^{-13} M target ctDNA. (B) The corresponding calibration curve of DPV peak current intensity *versus* target 134A concentration in oxygen-saturated PBS. Three DPV acquired by different determinations were averaged, and three repetitive experiments were executed. Error bars were the standard deviation of three tests. The blank was deducted from each value. (C) Peak current intensity of 11 replicates by DPV on the same chip. (D) Peak current intensity of seven different chips at 10^{-13} M concentrations of target 134A. The average was from three repetitive experiments (error bars, the standard deviation of three tests).

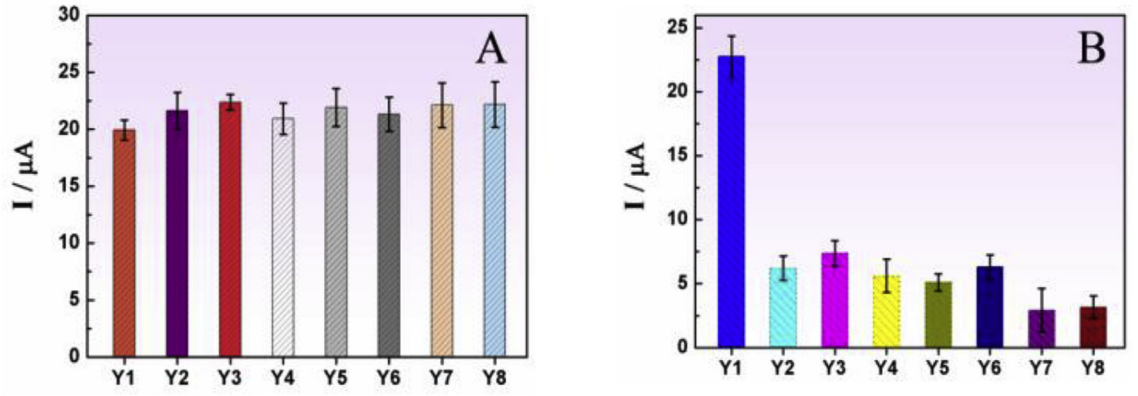

Fig. 5. Peak current intensity by DPV technique: (A) Detecting mutated ctDNAs (10^{-13} M) members on the DNA-probe chip. (B) Analyzing mutated ctDNAs family by the identifying chip with locked nucleic acid beacons. The average was from three repetitive experiments (error bars, the standard deviation of three tests).

the problem for the detection background, thus guaranteeing the specificity. It was imaginable that sensitivity and specificity of low-level ctDNA detection in tumor cells could be dramatically enhanced as a result of an identifying chip with and nucleic acid reactions.

3.2. Characterization of nano-composite fibers

Pt/ITO nanofibers-conjugated RCR product for ctDNA detections were successfully manufactured and characterized (Fig. 2). The average diameter of Pt/ITO nanofibers was approximately 150 nm (Fig. 2A), and TEM image of Pt/ITO nanofibers was shown in Fig. 2B, which demonstrated that Pt nanoparticles covered favorably in the outer layer of ITO nanofibers by in-line electrospinning, and EDS spectrum of Pt/ITO nanofibers exhibited their chemical composition. The RCR reaction of nucleic acids activated by target ctDNA was analyzed using agarose gel electrophoresis with ethidium bromide (EB) staining, which provided an efficient technical support for the 3D RCR-nanofibers (Fig. 2C). In Fig. 2D, Zeta potential (ZP) characterization indicated that this 3D bio-nanofiber could successfully self-assemble, nucleic acids as being a shell, Pt/ITO nanofiber as being a core.

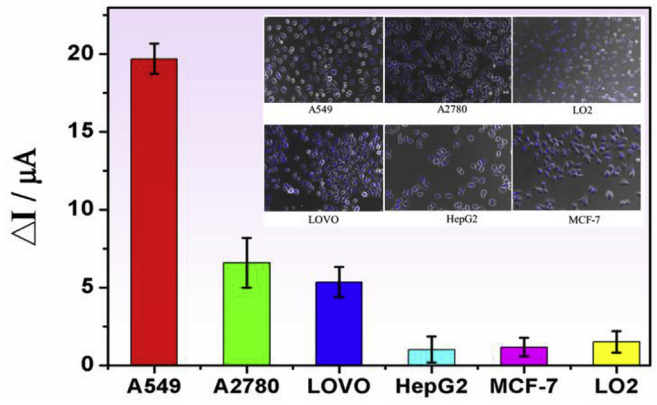

Fig. 6. Evaluation of coaxial sensing bio-amplifier for target ctDNA-134A within the cells (Cellular morphologies of A549, LOVO, MCF-7, HepG2 cells and LO2 cells were observed by inverted phase contrast microscopy).

Table 1
Detection of ctDNA-134A in the serum samples of peripheral blood by the coaxial sensing bio-amplifier (n = 3).

Samples	ctDNA-134A content added	ctDNA-134A content detected	Recovery (%)	RSD (%)
1	2.0×10^{-13} M	1.83×10^{-13} M	90.2 ± 0.63	10.7%
2	1.0×10^{-14} M	9.41×10^{-15} M	93.4 ± 0.76	9.35%
3	2.0×10^{-15} M	2.33×10^{-15} M	115.1 ± 0.83	11.3%

3.3. Electrochemical characterizations of Pt/ITO nanofibers

Cyclic voltammetry curves verified the catalytic performance of Pt/ITO nanofibers. As shown in Fig. 3A, Pt was modified on a glassy-carbon (GC) slice using cyclic voltammetry, and a clear redox peak was observed at −0.4 V, whereas the GC slice modified with Pt/ITO nanofibers was clearly observed at −0.43 V. The redox peaks indicated that Pt/ITO nanofibers had obvious redox electrocatalytic activity. The stability of Pt/ITO nanofibers was measured in 200 cycles (10 mV/s) in 0.1 M KOH of oxygen-saturation (Fig. 3B). The experimental data showed that the current density slightly decreased after 200 cycles but didn't affect the catalytic activity of Pt/ITO nanofibers. In Fig. 3C and D bio-nanofibers showed larger electrochemical impedance (EI) in contrast to Pt/ITO, due to the great conductivity of RCR products, demonstrating the successful formation of outer shell of nucleic acids.

3.4. Monitoring capability for target ctDNA

To evaluate the validity of this catalytic bio-amplifier, peak current intensity changes of DPV were measured at different concentrations of target ctDNA under the optimal reaction conditions (Fig. S2). This coaxial bio-amplifier demonstrated high sensitivity toward target ctDNA-134A detection with a dynamic range from 2.0×10^{-17} to 2.0×10^{-13} M (Fig. 4A) and showed remarkable selectivity to differentiate a single-base mismatched sequence from the perfectly complementary one. Linear regression follows the equation $I - I_0 = 4.797 \lg C_{ctDNA} + 8.158$ (Fig. 4B), the correlation coefficient (R^2) of the calibration curve was 0.996 (3σ), and the detection limit was calculated to be 5.1 aM. Reproducibility and stability are the important factors of biosensing applications. By implementing 11 replicates of 10^{-13} M target ctDNA-134A determinations under optimal conditions, on the same chip respectively modified eleven times, the relative standard deviation (RSD) was 7.3% (Fig. 4C). The stability of the coaxial sensing bio-amplifier was tested using seven different chips, and each test was measured three times for their error bars, the deviation was calculated less than 9.5% (Fig. 4D). There indicated that this coaxial bio-amplifier possessed the satisfying stability and repeatability.

3.5. Mutational analysis approach

Seven distinct point-mutation alleles of KRAS genes (Table S1) that are bound up with lung cancer were dynamically evaluated by this coaxial sensing bio-amplifier. It also demonstrated the significant sensitivity and specificity improvement than nanoparticles-based ctDNA detections, which resulted from the coaxial sensing-catalytic capability of SA-Pt/ITO nanofibers. Meanwhile, the method of DNA-probes (Fig. 5A) was compared with our approach of locked nucleic acid beacons (Fig. 5B) on the chips based on“covalent bridges lock effect”. This bio-amplifier displayed a high precision for ctDNA detection, due to the formation configurations of locked nucleic acid beacons and coaxial signal-amplification. In the N-type (3-endo) configuration of these beacons, there exist covalent bridges “lock” the ribose (Straarup et al., 2010; Riahi et al., 2014). Thus, relative to DNA-probes, locked nucleic acid beacons by the synergies of *in situ* 3BF and coaxial signal-amplification demonstrated remarkable recognition and strong appetency with target molecules in single-base mismatch or single base mutations.

3.6. Comparison experiments of different cells

A549, LOVO, MCF-7, HepG2 cells and LO2 cells were sequentially used to extract DNAs using a QIAmp®DNA Mini Kit, and DPV detection based on this catalytic bio-amplifier was put into effect. The extracted DNAs from LO2, MCF-7 and HepG2 cells didn't make any positive results (Fig. 6), in line with the reality that mutated KRAS sequences had hardly any discovery of in LO2, MCF-7, and HepG2 cells (Abbosh et al., 2017; Kaiser, 2010; Hu et al., 2018). The extracted DNAs from A549, LOVO, and A2780 cells were as the positive samples, comprising KSV mutants, which could clearly verify to have coupled the recognition chip. Simultaneously, the background signals in human serum had a mild decline by DPV responses for target ctDNA-134A, in contrast to those in PBS (Fig. S3), which might be owing to the interferences of complex media. The pretty recovery was obtained in the serum samples of peripheral blood (Table 1) by the standard addition method, demonstrating the applicability of this catalytic bio-amplifier to quantitative analysis of mutated ctDNAs.

4. Conclusions

In conclusion, coaxial sensing bio-amplifier was introduced to monitor the mutated ctDNAs within cells by dynamic self-assembly from target activation, the 3D amplifier exhibited high specificity and biostability for mutant ctDNAs, owing to the “covalent bridge effect” in the recognition chip with locked nucleic acid beacons. The proposed bioactive-nanofibers not only served as an underlying substrate for DNA amplification programming but also played signal enrichment-transduction, further reducing the detection limit of electrochemical methods. Coaxial amplifiers have a large surface area to volume ratio that could be applied as a versatile amplification platform to analyze the mutated ctDNAs, which showed remarkable performance in specificity and sensibility. Benefiting from the high specificity and sensitivity due to the “coaxial sensing” and “signal enrichment” effects, this powerful technique has a promising potential to more applied research in genetic target analysis of clinical diagnostics and mutation recognition.

Declaration of interests

The authors declare that they have no known competing financial interests or personal relationships that could have appeared to influence the work reported in this paper.

Acknowledgment

This work was supported by the National Science Foundation of China (21775061, 21705070, 21775063, 21535002), the Natural Science Foundation of Shandong Province (ZR2018JL012, ZR2016QZ001, ZR2017ZC0226).

Appendix A. Supplementary data

Supplementary data to this article can be found online at https://doi.org/10.1016/j.bios.2019.111414.

References

Abbosh, C., Birkbak, N.J., Swanton, C., et al., 2017. Nature 545, 446–451.
Angulo, I., Vadas, O., Garçon, F., Nejentsev, S., et al., 2013. Science 342, 866–871.
Catherine, R.L., Poh, Y.P., Peterson, B.K., Barrett, R.D.H., Larson, J.G., Jensen, J.D., Hoekstra, H.E., 2013. Science 339, 1–9.
Cutsem, E.V., Kohne, C.H., Lang, I., Folprecht, G., Nowacki, M.P., Cascinu, S., Shchepotin, I., Maurel, J., Cunningham, D., Tejpar, S., Schlichting, M., Zubel, A., Celik, I., Rougier, P., Ciardiello, F., 2011. J. Clin. Oncol. 29, 2011–2019.
Diehl, F., Schmidt, K., Choti, M.A., Romans, K., Goodman, S., Li, M., Thornton, K., Agrawal, N., Sokoll, L., Szabo, S.A., Kinzler, K.W., Vogelstein, B., Diaz, L.A., 2008. Nat. Med. 14, 985–991.
Garcia-Olmo, D.C., Dominguez, C., Garcia-Arranz, M., Anker, P., Stroun, M., Garcia-Verdugo, J.M., Garcia-Olmo, D., 2010. Cancer Res. 70, 560–567.
Gorgannezhad, L., Umer, M., Islam, M.N., Nguyen, N.T., Shiddiky, M.J.A., 2018. Lab Chip 18, 1174–1196.
Guan, Z., Jia, S., Zhu, Z., Zhang, M., Yang, C.J., 2014. Anal. Chem. 86 (5), 2789–2797.
Hanahan, D., Weinberg, R.A., 2011. Cell 144, 646–674.
Harley, C.B., 2008. Nat. Rev. Canc. 8, 167–179.
Hu, P., Zhang, S., Wu, T., Ni, D., Fan, W., Zhu, Y., Qian, R., Shi, J., 2018. Adv. Mater. 30 (1–9), 1801690.
Jabbari, H., Aminpour, M., Montemagno, C., 2015. ACS Comb. Sci. 17, 535–540.
Ji, X., Su, Z., Wang, P., Ma, G., Zhang, S., 2015. ACS Nano 9, 4600–4610.
Kaiser, J., 2010. Science 327, 1072–1074.
Li, J., Green, A.A., Yan, H., Fan, C., 2017. Nat. Chem. 9, 1056–1061.
Lin, M., Wang, J., Zhou, G., Wang, J., Wu, N., Lu, J., Gao, J., Chen, X., Shi, J., Zuo, X., Fan, C., 2015. Angew. Chem. Int. Ed. 54, 2151–2156.
Liu, Q., Ge, Z., Mao, X., Zhou, G., Zuo, X., Shen, J., Shi, J., Li, J., Wang, L., Chen, X., Fan, C., 2018a. Angew. Chem. Int. Ed. 57, 7131–7135.
Liu, X., Zhang, F., Jing, X., Pan, M., Liu, P., Li, W., Zhu, B., Li, J., Chen, H., Wang, L., Yan, H., Fan, C., et al., 2018b. Nature 559, 593–598.
Loscertales, I.G., Barrero, A., Guerrero, I., Cortijo, R., Marquez, M., Calvo, A.M.C., 2002. Science 295, 1695–1698.
Manuguerra, I., Grossi, G., Thomsen, R.P., Lyngsø, J., Pedersen, J.S., Kjems, J., Andersen, E.S., Gothelf, K.V., 2017. ACS Nano 11, 9041–9045.
Mohammed, A.M., Šulc, P., Zenk, J., Schulman, R., 2017. Nat. Nanotechnol. 12, 312–316.
Murtaza, M., Dawson, S.J., Tsui, D.W.Y., Gale, D., Forshew, T., Piskorz, A.M., Parkinson, C., Chin, S.F., Kingsbury, Z., Wong, A.S., Marass, F., Humphray, S., Hadfield, J., Bentley, D., Chin, T.M., Brenton, J.D., Caldas, C., Rosenfeld, N., 2013. Nature 497, 108–112.
Newman, A.M., Bratman, S.V., To, J., Wynne, J.F., Eclov, N.C., Modlin, L.A., Liu, C.L., Neal, J.W., Wakelee, H.A., Merritt, R.E., Shrager, J.B., Loo, B.W., Alizadeh, A.A., Diehn, M., 2014. Nat. Med. 20, 548–554.
Obernosterer, G., Martinez, J., Alenius, M., 2007. Nat. Protoc. 2, 1508–1514.
Quick, J., Grubaugh, N.D., Pullan, S.T., Claro, I.M., Smith, A.D., Gangavarapu, K., et al., 2017. Nat. Protoc. 12 (6), 1261–1276.
Riahi, R., Wang, S., Long, M., Li, N., Chiou, P.Y., Zhang, D.D., Wong, P.K., 2014. ACS Nano 8, 3597–3605.
Siravegna, G., Marsoni, S., Siena, S., Bardelli, A., 2017. Nat. Rev. Clin. Oncol. 14, 531–548.
Song, Y., Tian, T., Shi, Y., Liu, W., Zou, Y., Khajvand, T., Sili, Wa, Zhu, Z., Yang, C.J., 2017. Chem. Sci. 8, 1736–1751.
Straarup, E.M., Fisker, N., Hedtjärn, M., Lindholm, W., Rosenbohm, C., Aarup, V., Hansen, H.F., Ørum, H., Hansen, J.B.R., Koch, T., 2010. Nucleic Acids Res. 38, 7100–7111.
Stulz, E., Clever, G., Shionoya, M., Mao, C., 2011. Chem. Soc. Rev. 40, 5633–5639.
Wang, L., Deng, R., Li, J., 2015. Chem. Sci. 6, 6777–6783.
Xu, R.H., Wei, W., Krawczyk, M., Zhang, K., et al., 2017. Nat. Mater. 16, 1155–1162.
Zhang, Z., Wang, Y., Zhang, N., Zhang, S., 2016. Chem. Sci. 7, 4184–4189.
Zhang, Z., Jiao, Y., Zhu, M., Zhang, S., 2017. Anal. Chem. 89, 4320–4327.
Zhao, Y., Cao, X., Jiang, L., 2007. J. Am. Chem. Soc. 129, 764–765.